Available online at www.sciencedirect.com
SCIENCE DIRECT®
Journal of Molecular Catalysis A: Chemical 227 (2005) 269–278
JOURNAL OF MOLECULAR CATALYSIS A: CHEMICAL
www.elsevier.com/locate/molcata

Co and Mn impregnated MCM-41: their applications to vapour phase oxidation of isopropylbenzene

S. Vetrivel, A. Pandurangan*

Department of Chemistry, Anna University, Chennai 600 025, India

Received 30 August 2004; received in revised form 15 October 2004; accepted 19 October 2004
Available online 9 December 2004

Abstract

The mesoporous molecular sieves Si-MCM-41 and Al-MCM-41 (Si/Al = 99) were synthesized and their structures were elucidated by XRD, N_2-adsorption isotherm and TG-DTA technique. Monometallic cobalt and manganese oxides and also their bimetallic forms impregnated Si-MCM-41 and Al-MCM-41 catalysts were prepared by wet method and characterised by XRD, AAS, DRS-UV–vis and ESR techniques. The presence of Co^{3+} and Mn^{2+} in the mono and bimetal impregnated catalysts was evident through DRS studies. The analysis with DRS-UV–vis-spectroscopy showed independent existence of cobalt and manganese oxides in the bimetallic catalysts. AAS analysis showed higher loading of manganese than cobalt and the same difference was also observed for bimetal impregnated catalysts. The vapour phase oxidation of isopropylbenzene with CO_2-free air was studied over cobalt and manganese oxide impregnated Si-MCM-41 and Al-MCM-41 catalysts. Isopropylbenzene conversion increased with increase in temperature from 200 to 300 °C, but at 325 °C it decreased. Formation of coke has been noted at all the temperatures. Cumene hydroperoxide, 1,2-epoxy isopropylbenzene, acetophenone and styrene were the products observed in this reaction. Among the products, cumene hydroperoxide was found to have more selectivity than other products over all the catalysts. Both cobalt and manganese oxide impregnated catalysts were found to have nearly the same activity. The study of time-on-stream indicated decrease in conversion with stream due to coke formation.

Keywords: MCM-41; DRS-UV; ESR; Oxidation; Cumene and acetophenone

1. Introduction

The development of efficient catalysts for the selective oxidation of hydrocarbons by molecular oxygen has remained a difficult challenge to the catalytic science [1]. The dominant position of molecular oxygen as the oxidant for bulk chemical oxy-functionalizations is due to the fact that it is the only economically and environmentally friendly feasible oxidant for large scale processing. The oxidation of hydrocarbons catalyzed by transition metal complexes has been extensively studied [2–5]. Some of these oxidation reactions are important industrial processes in making commodity chemicals such as ethylbenzene hydroperoxide, *tert*-butyl hydroperoxide and cumene hydroperoxide [6]. The study of kinetics and mechanism of low temperature cumene oxidation with oxygen over the surface of simple metal oxides catalysts was carried out previously [7–9]. Hsu et al. discovered that the polymer-supported catalysts can catalyze the reaction between cumene and oxygen [10] to form cumene hydroperoxide via a free radical mechanism. They obtained the selectivity to cumene hydroperoxide 63%, but the conversion reported was only 6% under liquid phase reaction at 353 K. Kropf's et al. claimed that below 100 °C oxygen activation step responsible for the catalysis of cumene oxidation by metal-phthalocyanines via Kropf's mechanism [11–13]. Maksimov et al. dealt with low temperature cumene oxidation over the surfaces of Fe–O/ZrO_2, Fe–O/TiO_2 and Fe–O/Al_2O_3 complex oxides by sol–gel methods, and obtained poor (10–12%) cumene conversion and selectivity to cumene hydroperoxide (13%) [14]. In spite of the excellent

* Corresponding author. Tel.: +91 44 22203158; fax: +91 44 22200660.
E-mail address: pandurangan_a@yahoo.com (A. Pandurangan).

1381-1169/$ – see front matter © 2004 Published by Elsevier B.V.
doi:10.1016/j.molcata.2004.10.036

performance of these catalysts, there are some drawbacks. For instance, the catalysts exhibited slow decomposition at the reaction temperature of 363 K, and hence enhancing the reaction rate by employing these catalysts was impossible at high temperatures [15]. The main aim of this study is to use MCM-41 supported cobalt and manganese oxide catalysts for the oxidation of cumene using CO_2-free air as the oxidant, circumventing the above said drawbacks. As the support has mesopores, they are capable of holding metal oxides in nanodimensions with high catalytic activity. Catalyst precursor [16–19], support [20–22], preparation method [17–19,22–25] and metal loading [16,26] were observed to influence the oxidation behavior of cobalt and manganese catalysts. The effects of reaction temperature, weight hourly space velocity and time-on-stream on conversion and products selectivity were examined and the results discussed.

2. Experimental

2.1. Name of the chemicals used

The synthesized and impregnated MCM-41 catalysts were prepared by using sodium metasilicate ($Na_2SiO_3{\cdot}5H_2O$), cetyltrimethylammonium bromide ($C_{16}H_{33}(CH_3)_3N^+Br^-$), aluminium sulphate ($Al_2(SO_4){\cdot}18H_2O$), sulfuric acid ($H_2SO_4$), manganese acetate ($C_4H_6MnO_4{\cdot}4H_2O$), and cobalt nitrate ($Co(NO_3)_2{\cdot}6H_2O$). To study oxidation of isopropylbenzene to cumene hydroperoxide, the reagent isopropylbenzene was used. All the AR grade chemicals were purchased from E-Merck & Co.

2.2. Synthesis of catalysts

Al-MCM-41 (Si/Al = 99) was synthesized hydrothermally using a gel composition of SiO_2:0.01 Al_2O_3:0.2 CTAB:0.89 H_2SO_4:120 H_2O. In a typical synthesis, 21.2 g of sodium metasilicate dissolved in 80 ml deionized water was mixed with 0.67 g of aluminium sulphate (dissolved in 20 ml deionized water). This mixture was stirred for 30 min using a mechanical stirrer, and the pH of the solution was adjusted to 10.5 with constant stirring for another 30 min to form a gel. After that, 7.2 g of cetyltrimethylammonium bromide was added drop by drop (25 ml/h) through the syringe infusion pump so that the gel was changed into suspension. The suspension was transferred into a Teflon-lined steel autoclave and heated to 160 °C for 48 h. After cooling to room temperature, the product formed was filtered, washed with deionized water and finally calcined in flowing air at 550 °C for 6 h. Si-MCM-41 was also synthesized in a similar manner without aluminium sulphate.

2.3. Preparation of Co and Mn impregnated catalysts

Fifty millilitre of 0.3 M manganese acetate/cobalt nitrate solution was mixed with 3 g of Si-MCM-41 or Al-MCM-41 to prepare the impregnated catalysts by stirring 6 h. The residue was filtered and gently washed with deionized water in order to remove metal ions adsorbed on the external surface. The filtrate was dried under reduced pressure, and finally calcined in air at 550 °C for 6 h.

2.4. Physico-chemical characterization

The aluminium content in Al-MCM-41 was determined using ICP-AES with allied analytical ICAP 9000. The Mn and Co content in Si-MCM-41 and Al-MCM-41 was estimated using AAS (GBC 932 plus) by flowing acetylene and air at a rate of 1.85 and 13.1 l/min, respectively. XRD analysis was performed on a Siemens D5005 stereoscan diffractometer equipped with liquid nitrogen-cooled germanium solid-state detector using Cu Kα radiation. The samples were scanned between 0.5° and 8.5° (2θ) in steps of 0.02° with the counting time of 5 s at each point. ASAP-2010 volumetric adsorption analyzer manufactured by the Micromeritics Corporation (Norcross, GA) was used to determine the specific surface area of the catalysts at liquid nitrogen temperature. Before the measurement, each sample was degassed at 623 K at 10^{-5} Torr overnight in an out gassing station of the adsorption apparatus. The full adsorption–desorption isotherm was obtained using BET method at various relative pressures; the pore size distribution and wall thickness were calculated from the nitrogen adsorption–desorption isotherms using the BJH algorithm (ASAP-2010 built-in software from Micromeritics).

Thermal decomposition of the as-synthesized samples was examined on Rheometric scientific (STA 15 H^+) thermo balance. An amount of 10–15 mg of as-synthesized MCM-41 catalyst was placed in a platinum pan and heated from 30 to 1000 °C at a heating rate of 20 K min^{-1} in air with a flow rate of 50 ml min^{-1}. The co-ordination environment of cobalt and manganese containing MCM-41 catalyst was examined by diffuse reflectance UV–vis spectroscopy. The spectra were recorded between 200 and 800 nm on a Shimadzu (UV–vis spectrophotometer Model 2101 PC) using $BaSO_4$ as the reference. The spectra were recorded at room temperature in the presence of air. The co-ordination environment of manganese was analyzed by ESR technique (Varian E112 spectrometer operating in the X-band 9 GHz region). DPPH was used as the reference to mark the *g* value. The relative ESR intensities were calculated by double integration of the recorded ESR signal.

2.5. Experimental procedure for oxidation of isopropylbenzene

The oxidation of isopropylbenzene with CO_2-free air was carried out in a fixed bed down flow quartz reactor under atmospheric pressure in the temperature range of 200–325 °C in steps of 25 °C. Prior to the reaction, the reactor packed with 0.3 g of the catalyst was preheated in a tubular furnace equipped with a thermocouple. The isopropylbenzene

was fed into the reactor using a syringe infusion pump at a predetermined flow rate. The oxidation of isopropylbenzene was carried out and the products mixture was collected for a time interval of 1 h. The products were analyzed by gas chromatography (Hewlett-Packard 5890A) equipped with Flame Ionization Detector and PONA column. The identification of products was also performed on a Shimadzu GC–MS-QP1000EX gas chromatograph–mass spectrometer. No significant isopropylbenzene conversion was observed when the reaction was carried out without catalyst indicating that there is no thermal effect on conversion. All the catalysts were regenerated by burning away the coke deposit formed on them from the previous reaction temperature by passing a stream of pure dry air at a temperature of 500 °C for 6 h. The catalysts were used continuously to study the effect of various parameters, viz., temperature, weight hourly space velocity and time-on-stream.

3. Results and discussion

3.1. X-ray diffraction study

The X-ray diffraction spectrum of MCM-41 (Fig. 1A) samples contains a sharp d_{100} reflection line in the 2θ range 1.9–2.4°. Additionally two broad peaks at 2θ range 3.6–4.5° are obtained. These peaks have been attributed to the broadening effect of higher reflection lines due to small size [27]. The physico-chemical properties of these mesoporous materials are summarized in Table 1. The hexagonal unit cell parameter (a_0) was calculated using the formula $a_0 = 2d_{100}/\sqrt{3}$, which was obtained from the peak in the XRD pattern by Bragg's equation ($2d \sin\theta = \lambda$, where $\lambda = 1.54$ Å for the Cu Kα radiation). The value of a_0 was equal to the internal pore diameter plus one pore wall thickness. The existence of the same peaks in the Al-MCM-41 catalyst suggests that the long-range order is sustained even after the incorporation of metal. These peaks was broadened and shifted slightly to higher angle with increasing metal content, although the hexagonal structure still remained intact. These results suggest that the regularity of the mesoporous structure decreased and the pore size become slightly narrower with the introduction of metals [28]. After calcination (Fig. 1B), the 1 0 0 reflection shift to a higher value indicating a contraction of the lattice caused by template removal and subsequent condensation of silanol groups.

Fig. 1C shows the XRD patterns of the manganese and cobalt impregnated catalysts. The intensity of the patterns due to 1 0 0 plane decreased and that of 1 1 0 and 2 0 0 planes disappeared owing to radiation diffusion. This can be attributed to the nanosize of the impregnated particles present in the pores.

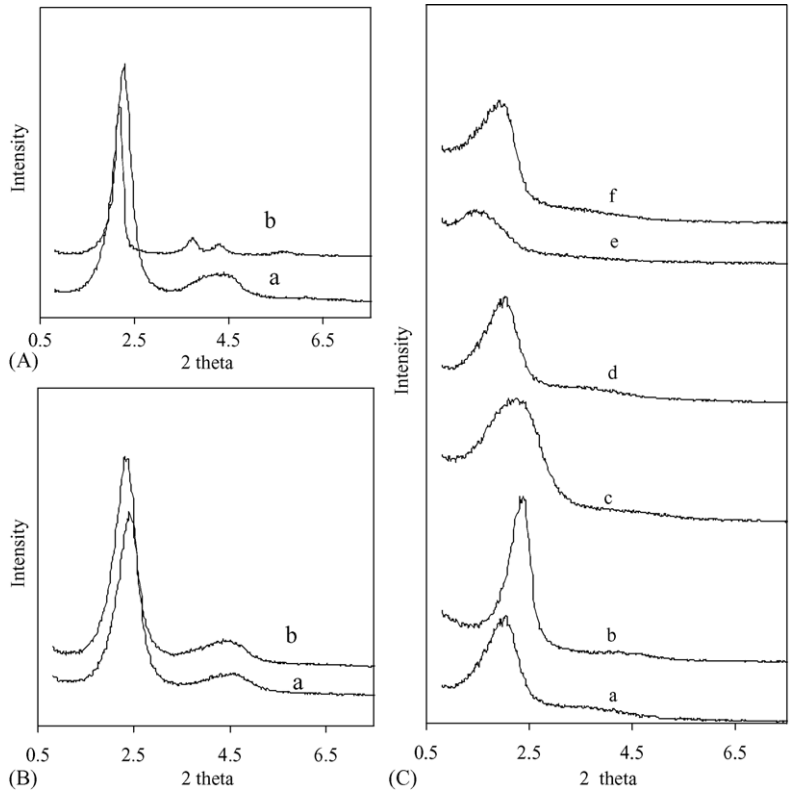

Fig. 1. XRD of (A) as-synthesized, (B) calcined (a) Si-MCM-41, (b) Al-MCM-41 (99) and (C) after impregnation of (a) Co-MCM-41, (b) Co–Al-MCM-41 (99), (c) Mn-MCM-41, (d) Mn–Al-MCM-41 (99), (e) Mn–Co-MCM-41, (f) Mn–Co–Al-MCM-41 (99).

Table 1
Structure parameters for the Al, Mn and Co containing MCM-41 type materials

Catalysts	d_{100}-spacing value (Å)			Unit-cell parameter (Å)		
	A	B	C	A	B	C
Si-MCM-41	40.16	36.21	–	46.37	41.81	–
Al-MCM-41 (99)	38.75	36.82	–	44.74	42.52	–
Co-MCM-41	–	–	42.89	–	–	49.53
Co–Al-MCM-41 (99)	–	–	36.82	–	–	42.52
Mn-MCM-41	–	–	43.06	–	–	49.72
Mn–Al-MCM-41 (99)	–	–	48.12	–	–	55.57
Mn–Co-MCM-41	–	–	61.30	–	–	70.84
Mn–Co–Al-MCM-41 (99)	–	–	50.08	–	–	57.83

A = as-synthesized, B = calcined and C = after impregnation.

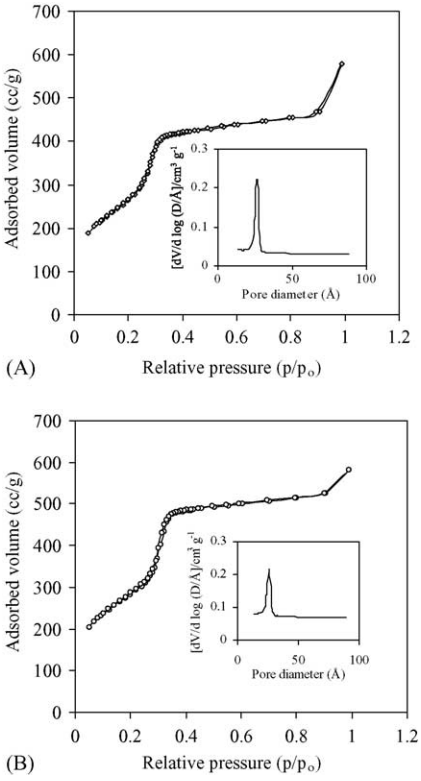

Fig. 2. N_2 adsorption isotherm of calcined (A) Si-MCM-41 and (B) Al-MCM-41 (99).

3.2. Textural property

Nitrogen adsorption–desorption isotherms for the calcined samples and their corresponding pore size distribution calculated using the BJH method based on the adsorption isotherms are presented in Fig. 2A and B. It is observed that there are three distinct well-defined stages in the isotherm. The initial increase in nitrogen uptake at low P/P_0 may be due to monolayer adsorption on the pore walls, a sharp steep at intermediate P/P_0 may indicate the capillary condensation in the mesopores and a plateau portion at high P/P_0 associated with multilayer adsorption on the external surface of the catalysts. All the catalysts show a characteristic step around $P/P_0 \approx 0.3$ indicating the mesoporous nature of the materials [29]. The sharpness and height of the capillary condensation step are the indications of pore size uniformity. Deviations from sharp and well-defined pore filling step are the indications of increase in pore size heterogeneity. A steep rise in the adsorbed amount was observed at relative pressures in the range 0.24–0.32 Pa, being caused by capillary condensation of nitrogen in the mesopores. This rise become more gentle and was shifted to lower relative pressure with metal content, which suggests that the pore size was narrowed and distributed. The specific surface area of samples determined by the BET surface area lies in the range of 949–978 m^2/g for Si-MCM-41 and Al-MCM-41. The surface area, pore size, pore volume, and wall thickness are given in Table 2. It is observed that the surface area, pore diameter, and pore volume was higher for Al-MCM-41 than Si-MCM-41

3.3. Thermal analysis

Thermogravimetric analysis of the catalysts shows distinct weight losses that depend on framework composition. Fig. 3 exhibits three distinct stages of weight loss. The first weight loss is due to desorption of water ∼11.43–11.52% was observed between 50 and 150 °C. The second stage between 150 and 350 °C, corresponding to a weight loss of ∼32.49–27.60%, is due to the decomposition of the surfactant species. Finally, the weight loss of ∼8.44–11.93% from 350 to 550 °C is assigned to condensation of adjacent silanol groups to form a siloxane bond [30]. The total weight loss up

Table 2
Physico-chemical characterization of Al containing MCM-41 type materials

Catalysts	N_2-adsorption isotherm				TG-DTA weight loss (wt.%)			
	Surface area (m^2 g^{-1})	Pore size (Å)	Pore volume (cm^3/g)	Wall thickness (Å)	Total	50–150 °C	150–350 °C	350–550 °C
Si-MCM-41	949	30.1	0.95	16.27	52.36	11.43	32.49	8.44
Al-MCM-41 (99)	978	32.7	0.97	12.04	51.05	11.52	27.60	11.93

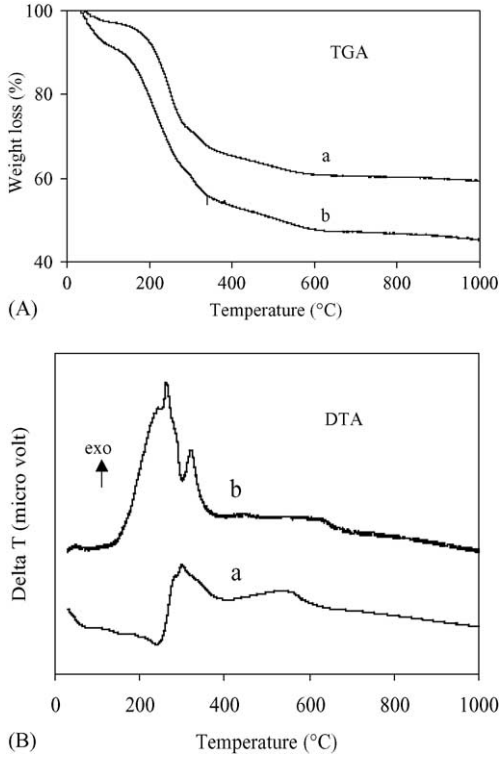

Fig. 3. TG-DTA curve of as-synthesized (A) Si-MCM-41, (B) Al-MCM-41 (99).

to 1000 °C of the Si-MCM-41 and Al-MCM-41 samples are in the range 52.36–51.05%.

The DTA of the as-synthesized samples was carried out between 30 and 1000 °C at a heating rate of 20 K min^{-1} in air. The DTA trace of Si-MCM-41 shows two broad exotherms: the first at 230 °C and the second at 450 °C. They are assigned to decomposition of template and condensation of defective sites, respectively. The DTA trace due to Al-MCM-41 shows two exothermic peaks between 200 and 400 °C. The intense first exotherm is due to loss of template bonded to silicon sites, and the second minor exotherm due to template bonded to aluminium sites. This is the evidence for condensation of defective sites above 400 °C but it is not as high as Si-MCM-41. From this study it can be revealed that the presence of defective sites is more for Si-MCM-41 than Al-MCM-41.

3.4. DRS-UV–vis spectroscopy

The DRS-UV–vis analysis of Mn and Co impregnated MCM-41 and Al-MCM-41 catalysts were carried out between 200 and 800 nm covering the entire ultraviolet and visible region. The spectra are presented in Fig. 4. Mn-MCM-41 and Mn–Al-MCM-41 produce less resolved absorption band with maxima at 270 and 500 nm. These absorption maxima coincide with the reports in the literature [31]. As Mn is in

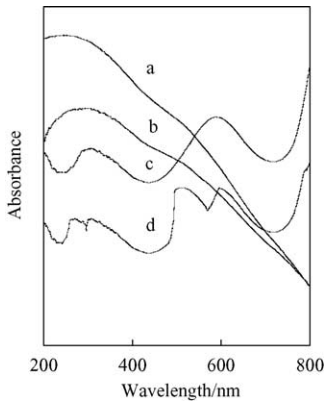

Fig. 4. DRS-UV–vis spectra of calcined (a) Mn-MCM-41, (b) Mn–Al-MCM-41 (99), (c) Co–Al-MCM-41 (99), (d) Mn–Co–Al-MCM-41 (99).

the non-framework it is to have an octahedral environment of oxygen. As Mn is in 2+ oxidation state shown by ESR spectroscopy, it is to have ^6S groundterm. As ^6S does not have crystal field components, the electronic excitations are forbidden, but there may be spin orbit interactions, as reported in the literature [32] with which some transitions may have allowance. In conformation of this, in the DRS-UV spectra of Mn-MCM-41 and Mn–Al-MCM-41 the absorption bands are absorbed. But they cannot be due to $^6A_{1g} \rightarrow {}^4T_{2g}$ and charge transfer transition as reported in the literature [33,34]. The DRS-UV spectrum of Co–Al-MCM-41 is shown in the same figure. There are two absorption maxima, one at 280 nm and the other at 580 nm corresponding to cobalt in octahedral environment. The latter one is assigned to $^5T_{2g} \rightarrow {}^5E_g$ transition and the former to charge transition. The absorption shoulder between 300 and 400 nm is assigned to electronic transition of Co^{3+} in disordered tetrahedral environment.

The DRS-UV spectrum of Mn–Co–Al-MCM-41, shown in the same figure, exhibits absorption maxima, which are the combination of absorptions due to Mn–Al-MCM-41 and Co–Al-MCM-41. Based on this observation, it could be concluded that both Mn and Co oxides are of separate independent moieties without forming any new chemical compound.

3.5. ESR spectroscopy

Fig. 5 shows X-band ESR spectra of calcined samples recorded at liquid nitrogen temperature. There are six hyperfine lines centered around $g = 2.00$ (Table 3) corresponding to Mn^{2+} in octahedral environment. Similar observations were noted for Mn-MCM-41 [35] and MnAPO-5 [36] with the Mn species located at non-framework positions. The splitting of the sextet increases from 3010 to 3550 G. Meanwhile, the peak-to-peak line-width increases and the line height decreases. These observations indicate that the Mn^{2+} ions are strongly interacting with their environment in the octahedral

Table 3
Elemental analysis of Mn and Co containing MCM-41 catalysts

Catalysts	AAS results			*g* value of ESR
	Theoretical (ppm)	Experimental (ppm)		
		Mn	Co	
Co-MCM-41	5.67	–	5.06	–
Co–Al-MCM-41 (99)	5.67	–	4.57	–
Mn-MCM-41	5.67	5.12	–	2.0018
Mn–Al-MCM-41 (99)	5.67	5.00	–	2.0005
Mn–Co-MCM-41	11.45	4.97	4.97	–
Mn–Co–Al-MCM-41 (99)	11.45	6.28	4.33	–

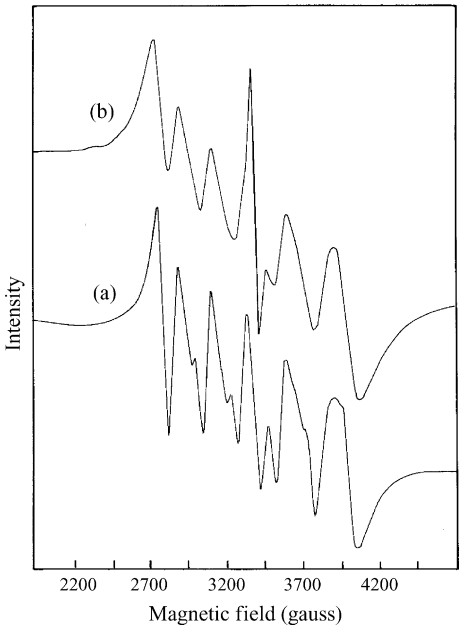

Fig. 5. ESR spectra of calcined (a) Mn-SiMCM-41, (b) Mn–Al-MCM-41 (99).

coordination, which is consistent with non-framework position [26].

3.6. Influence of temperature

The vapour phase oxidation of isopropylbenzene over cobalt oxide impregnated Si-MCM-41 and Al-MCM-41 in the temperature range 200–325 °C was studied with CO_2-free air as the oxidant. The selectivity to cumene hydroperoxide (CHP), 1,2-epoxy isopropylbenzene (1,2-EIPB), acetophenone (AP) and styrene were the products observed. Co^{3+} catalyses oxidation of cumene by abstracting the tertiary hydrogen to form cumene radical as shown in the following reaction scheme. This mechanism was also reported in the literature [37–39]. The cumene radical reacts with molecular oxygen to produce alkyl peroxide. The peroxide in turn abstracts hydrogen from cumene to form cumene hydroperoxide. The arolkyl hydroperoxide is decomposed catalytically to yield acetophenone and 1,2-EIPB.

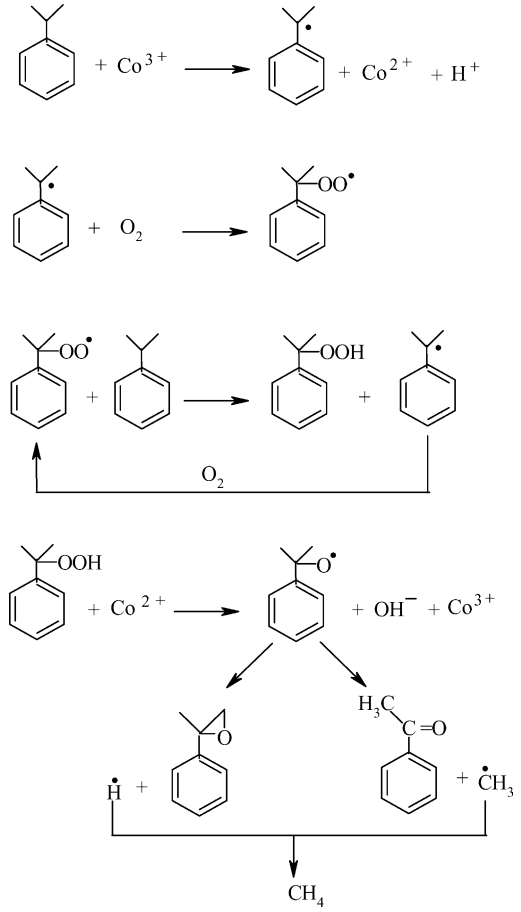

The conversion increased from 200 to 300 °C, but at 325 °C it slight decreased. As coke formation was observed at all the temperatures, and more favored with increase in temperature, the increase in conversion between 200 and 300 °C was not high. Nearly similar values of conversion at each temperature over all the catalysts might be due to similar level of dispersion of cobalt oxide on the catalyst surface. It is once again supported by nearly similar level of impregnation of cobalt oxide as evidenced from AAS analysis (Table 3). In order to test whether the carbon deposits or sintering of metal oxide caused catalyst deactivation, the spent catalyst, Co-MCM-41, was again tested for activity under identical conditions after activation. Before activation conversion of cumene was 50.1% and the same used catalyst after activation

gave 49.2% conversion, proving thus only carbon deposit as the cause for catalyst deactivation.

Among the products the selectivity to CHP was higher than the others at all the temperatures studied. Its selectivity increased from 200 to 300 °C, but at 325 °C it decreased. The decomposition of CHP might not be entirely free, but to be assisted by the catalyst, since the selectivity was not increased at 325 °C. Similar to conversion, CHP selectivity showed similar trend of increase with increase in temperature over all the catalysts up to 300 °C. The selectivity to 1,2-EIPB and acetophenone decreased with increase in temperature. The selectivity of 1,2-EIPB was higher than acetophenone at lower temperatures, but at higher temperature the reverse trend is appeared. But the decrease in selectivity of acetophenone was not higher compared to 1,2-EIPB.

The increase in the selectivity of CHP with increase in temperature was equal to decrease in the selectivity of 1,2-EIPB and acetophenone with increase in temperature. Hence, the latter products might be obtained from the decomposition of CHP. The catalyst might assist the formation of these two products also revealed the decomposition of CHP. At higher temperature, the decomposition of CHP was not favored due to less adsorption of it on the catalyst surface. The less selectivity of CHP at 325 °C contradicts this view, as the expected value was to be high. The less value might be due to formation of styrene with more selectivity directly from cumene via radical mechanism as shown in the following reaction scheme:

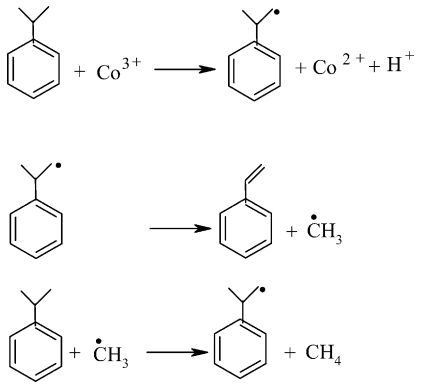

At high temperature, Co^{3+} is expected to abstract electron from the methyl group of cumene to form arolkyl radical. The arolkyl radical decomposes to produce styrene. The Co^{2+} formed in this reaction will catalyse arolkyl hydroperoxide as given in the previous mechanism. Formation of styrene directly from cumene was also established by passing the latter over the catalyst in the absence of air. Styrene was obtained with 7.8% yield at 300 °C. The same trends of selectivity for all the products over all the catalysts suggest occurring of similar mechanism for different reactions. As the conversion over all the catalysts nearly remained the same, the protonic sites of the catalyst of Co–Al-MCM-41 might not have any influence in this reaction. The reaction was also studied freshly over silica [40] supported cobalt oxide (0.3 M loading). When isopropylbenzene was passed over this catalyst, to our surprise, at 250, 275, 300 and 325 °C, the conversions were found to be 4.8, 9.2, 16.4 and 11.3% which are very low compared to MCM-41 supported catalysts. It might be due to large size of the metallic oxide.

Under the same conditions the reaction was also studied over Mn-MCM-41 and Mn–Al-MCM-41. The conversion showed similar trend as observed with Co catalysts: the conversion increased from 200 to 300 °C but decreased afterwards. Compared to Co catalysts the Mn catalysts gave slightly high conversion. It might be due to high loading of manganese oxide compared to Co catalysts. AAS analysis of these catalysts (Table 3) showed almost similar level of loading as that of Co, therefore small increase in conversion might be attributed to size of manganese oxides. The selectivity to CHP also showed similar trend of increased with increase in temperature up to 300 °C and decrease at 325 °C as that of the previous set of the catalysts. Similarly, the selectivity patterns of 1,2-EIPB, acetophenone and styrene were also retained the same in this catalysts as that of the previous ones in the temperature range studied. Hence there might be high-level dispersion of manganese oxides in this catalysts. Hence the mechanism detailed for Co catalysts would be similarly operating over Mn catalysts.

The reaction was also studied with binary Mn and Co oxide impregnated catalysts (Mn–Co-MCM-41 and Mn–Co–Al-MCM-41). The conversion and products selectivity was higher (Fig. 6) than the mono metal oxide catalysts at all temperature. Hence there might be higher loading of metal oxides. Again the metal oxide particles might also be in a state of fine dispersion to exhibit activity similar to that of either Mn or Co oxide impregnated catalysts. The selectivity to CHP, 1,2-EIPB, acetophenone and styrene appeared to have similar trend as obtained with mono metal oxide catalysts. Hence the mechanism of the reaction might remain the same with these catalysts too. Therefore, the active sites of the catalysts might not be different from the mono metal oxide catalysts suggesting absence of any new chemical compound formation in bimetallic oxide catalysts. The metal oxide particles might therefore retain their identity in the range of temperatures studied.

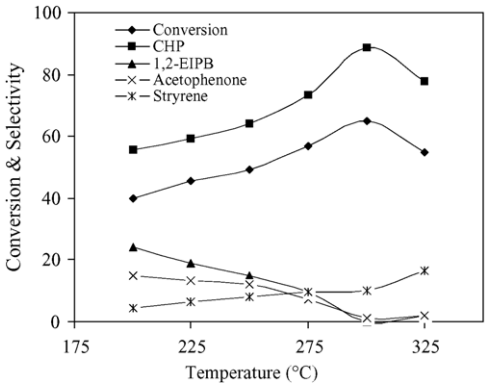

Fig. 6. Effect of temperature on the conversion and products selectivity over Mn–Co-MCM-41.

Table 4
Oxidation of cumene: variation with WHSV

Catalysts	WHSV (h^{-1})	Conversion (wt.%)	Products selectivity (%)				
			CHP	1,2-EIPB	AP	Styrene	Others
Co-MCM-41	2.9	50.1	81.3	3.7	5.7	8.7	1.2
	5.8	46.5	67.3	9.8	7.9	5.6	9.4
	8.6	41.2	60.1	16.7	8.1	3.5	11.6
	11.5	37.8	57.1	28.9	10.3	2.9	0.8
Co–Al-MCM-41 (99)	2.9	45.5	64.7	4.1	5.8	17.1	8.3
	5.8	40.3	54.2	11.6	8.8	13.5	11.9
	8.6	37.7	47.5	19.1	10.6	11.3	11.5
	11.5	34.9	44.3	26.6	13.1	8.6	7.4
Mn-MCM-41	2.9	59.6	85.9	0	1.5	12.6	0
	5.8	55.8	80.2	5.8	4.6	8.1	1.3
	8.6	51.1	72.8	8.6	9.5	6.2	2.9
	11.5	45.8	66.8	13.9	12.2	5.5	1.6
Mn–Al-MCM-41 (99)	2.9	53.8	77.8	2.5	3.2	16.3	0.2
	5.8	50.0	70.3	8.1	5.5	13.8	2.3
	8.6	47.5	63.8	10.5	7.5	12.1	6.1
	11.5	43.8	54.5	16.6	14.9	8.8	5.2
Mn–Co-MCM-41	2.9	64.9	88.7	0	1.3	10.0	0
	5.8	60.1	84.2	3.8	5.1	6.9	0
	8.6	57.5	78.1	6.6	9.4	4.2	1.7
	11.5	54.6	70.0	11.3	13.0	5.4	0.3
Mn–Co–Al-MCM-41 (99)	2.9	58.2	86.5	1.3	1.5	10.7	0
	5.8	55.0	77.7	4.5	8.1	8.0	1.7
	8.6	50.9	71.7	7.8	11.0	6.0	2.9
	11.5	45.8	66.6	14.0	13.0	3.3	3.1

Reaction conditions: 0.3 g of catalyst, temperature 300 °C, and flow rate of molecular oxygen 0.021 mol h^{-1}.

3.7. Influence of isopropylbenzene content in the feed

The effect of isopropylbenzene content in the feed on conversion and products selectivity over the cobalt oxide impregnated catalysts was studied at 300 °C. The reaction results are presented in Table 4. Conversion decreased with increase in the isopropylbenzene content over all the catalysts. Since the flow rate of molecular oxygen was 0.021 mol h^{-1} from CO_2-free air, nearly the same contact time for isopropylbenzene over the active sites of the catalyst irrespective of its content in the feed was expected. The conversion decreased, it might be due to increase in the formation of molecular clusters of isopropylbenzene with increase in its content in the feed. These molecular clusters prevent chemisorption and subsequent decomposition of isopropylbenzene over the active sites.

The selectivity of CHP decreased with increase in the isopropylbenzene content in the feed over all the catalysts. The high selectivity at lower content of isopropylbenzene might be due to decrease in the amount of Co(III) sites to chemisorption and subsequent decomposition of CHP. The less amount of Co(III) was due to more conversion of it to Co(II) due to more formation of isopropylphenyl free radical. The decrease in the selectivity with increase in the content of isopropylbenzene in the feed very well proved more and more formation of molecular clusters with increase in the isopropylbenzene content. As there might be less adsorption of isopropylbenzene, there might be more availability of Co(III) states in order to chemisorb, decompose and reduce the selectivity of CHP. The increase in the selectivity of 1,2-EIPB and acetophenone also conformed the above suggestion for formation of molecular clusters at high isopropylbenzene content. Formation of styrene with more selectivity at lower isopropylbenzene content in the feed and less selectivity at higher isopropylbenzene content in the feed also provided support for the increased formation of molecular clusters with increase in the isopropylbenzene content.

The effect of isopropylbenzene content in the feed on conversion and products selectivity was examined over Mn-MCM-41 and Mn–Al-MCM-41 catalysts. The results are presented in Table 4. The conversion decreased with increase in the isopropylbenzene content over all the catalysts. This trend is similar to the previous set of catalysts as discussed in the previous sections. The conversion is slightly high compared to Co catalysts. The selectivity to CHP decreased with increase in the isopropylbenzene content in the feed over all the catalysts similar to the previous set of catalysts. The increase in the selectivity of 1,2-EIPB and acetophenone, and decrease in the selectivity of styrene over all the catalysts could also be accounted based on the formation of molecular clusters as discussed before. The results of the effect of WHSV on conversion was studied over Mn–Co-MCM-41 and Mn–Co–Al-MCM-41, are also presented in the same

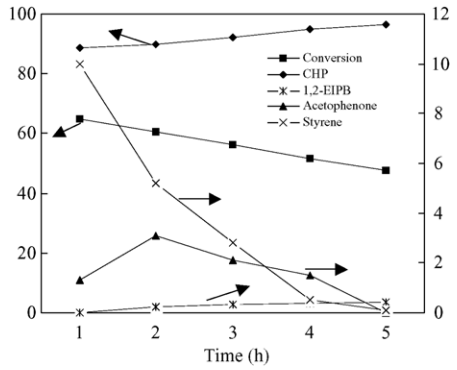

Fig. 7. Effect of time-on-stream on conversion and products selectivity over Mn–Co-MCM-41.

table. The conversion was higher for each WHSV than the mono metal oxide catalysts, so their cumulative effect due to their independent existent on conversion is clearly evident. The selectivity to the products showed similar variation as that of mono metal oxide catalysts with increase in WHSV.

3.8. Influence of time-on-stream

The effect of time-on-stream on conversion and products selectivity was studied by streaming the bimetallic oxide (Mn–Co-MCM-41) catalyst for 5 h. The study was carried out at 325 °C with the flow rate of isopropylbenzene 2.9 h^{-1} (WHSV) and molecular oxygen was 0.021 mol h^{-1} from CO_2-free air, and the results are illustrated in Fig. 7. The conversion decreased with increase in stream due to coke formation. The coke was also estimated after the end of time-on-stream study. It was found to be 19.8%. The selectivity to CHP increased with increase in stream due to blocking of active sites, which could assist its decomposition to 1,2-EIPB and acetophenone. Though the selectivity of 1,2-EIPB and acetophenone followed the same trend as in the earlier study, the selectivity to 1,2-EIPB increased with increase in stream and to acetophenone decreased with increase in stream. This observation suggests existence of acid sites of different strengths.

Though both the products are formed by the decomposition of CHP, the formation of acetophenone might be requiring acid sites of more strength than 1,2-EIPB, as the more active sites would be rapidly blocked by coke. The selectivity to acetophenone decreased with increase in stream. Since the formation of 1,2-EIPB required weak acid sites, its selectivity increased with increase in stream, as these sites might not be blocked by coke. As the strong acid sites are more and more blocked with increase in stream, there might be more transport of CHP to weak acid sites to yield 1,2-EIPB with more selectivity. The selectivity to styrene decreased with increase in stream due to coke formation. This decrease suggests requiring of more active sites for its formation.

4. Conclusions

This study illustrates cobalt and manganese oxides supported on MCM-41 and Al-MCM-41 are active to functionalization of isopropylbenzene in the vapour phase using CO_2-free air as the oxidant. This study is more advantageous than liquid phase reactions which use peroxide oxidants. The reaction is continuous and very simple to carry out. The major products are cumene hydroperoxide, 1,2-epoxy isopropylbenzene, acetophenone and styrene. Significant conversion is obtained from 200 to 300 °C. The reaction was repeated thrice at 325 °C to examine sintering of metal oxides, but the conversion remains the same for the three experiments illustrating avoidance of sintering. One important observation in the study is the formation and the high selectivity of cumene hydroperoxide. High conversion, and selectivity to cumene hydroperoxide was retained even for 5 h stream. Presence of protonic sites in the Al-MCM-41 does not seem to be harmful in the study. Harmless air is used as an oxidant as a substitute for H_2O_2.

References

[1] L.I. Simandi, Catalytic Activation of Dioxygen by Metal Complexes, Kluwer Academic Publishers, Dordrecht, 1992, p. 1.
[2] M. Fetizon, W.J. Thomas (Eds.), The Role of Oxygen in Improving Chemical Process, The Royal Society of Chemistry, Cambridge, 1993.
[3] G.W. Parshall, S.D. Ittel, Homogeneous Catalysis, 2nd ed., Wiley, New York, 1992.
[4] D.T. Sawyer, Oxygen Chemistry, Oxford University Press, Oxford, 1991.
[5] D.H.R. Barton, A.E. Martell, D.T. Sawyer (Eds.), The Activation, of Dioxygen and Homogeneous Catalytic Oxidation, Plenum Press, New York, 1993.
[6] K. Weissermel, H.–J. Arpe, in: C.R. Lindley (Ed.), Industrial Organic Chemistry, 2nd ed., VCH, New York, 1993.
[7] H.W. Meville, S. Richards, J. Chem. Soc. 3 (1954) 944.
[8] H. Hock, H. Kropf, J. Prak. Chim. 9 (1959) 173.
[9] N.M. Emanuel (Ed.), Teoria i Practica Gidrophaznogo Okyslenia, Nauka, Moskva, 1974, p. 330.
[10] Y.F. Hsu, M.H. Yen, C.P. Cheng, J. Mol. Catal. 105 (1996) 137.
[11] H. Kropf, Liebigs Ann. 637 (1960) 73.
[12] H. Hock, H. Kropf, J. Prak. Chim. 13 (1961) 20.
[13] H. Kropf, W. Knabjohann, Liebigs Ann. 739 (1970) 95.
[14] Y.V. Maksimov, I.P. Suzdalev, M.V. Tsodikov, V.Y. Kugel, O.V. Bukhtenko, E.V. Slivinsky, J.A. Navio, J. Mol. Catal. A: Chem. 105 (1996) 167.
[15] Y.F. Hsu, C.P. Cheng, J. Mol. Catal. A: Gen. 120 (1997) 109.
[16] M.P. Rosynek, C.A. Polanky, Appl. Catal. 73 (1991) 97.
[17] E. van Steen, G.S. Sewell, R.A. Makhothe, C. Micklethwaite, H. Manstein, M. De Lange, C.T. O'Connor, J. Catal. 162 (1996) 220.
[18] L.B. Backman, A. Rautiainen, A.O.I. Krause, M. Lindblad, Catal. Today 43 (1998) 11.
[19] Y. Okamoto, K. Nagata, T. Adachi, T. Imanaka, K. Inamura, T. Takyu, J. Phys. Chem. 95 (1991) 310.
[20] G.S. Sewell, E. van Steen, C.T. O'Connor, Catal. Lett. 37 (1996) 225.
[21] S. Bessel, Appl. Catal. A: Gen. 96 (1993) 253.
[22] R.C. Reuel, C.H. Bartholomew, J. Catal. 85 (1984) 63.
[23] K.E. Coulter, A.G. Sault, J. Catal. 154 (1995) 56.

[24] R. Srinivasan, R.J. de Angelish, P.J. Reucroft, A.G. Dhere, J. Bentley, J. Catal. 116 (1989) 144.
[25] H. Ming, B.G. Baker, Appl. Catal. A: Gen. 123 (1995) 23.
[26] S. Vetrivel, A. Pandurangan, Appl. Catal. A: Gen. 264 (2004) 243.
[27] P.T. Tanev, T.J. Pinnavaia, Science 267 (1995) 865.
[28] J.S. Beck, J.C. Vartuli, W.J. Roth, M.E. Leonowicz, C.T. Kresge, K.D. Schmitt, C.T.W. Chu, D.H. Olson, E.W. Sheppard, S.B. Mccullen, J.B. Higgins, J.C. Schlinker, J. Am. Chem. Soc. 114 (1992) 10834.
[29] S.J. Gregg, K.S.W. Sing, Adsorption, Surface Area and Porosity, 2nd ed., Academic Press, New York, 1982.
[30] M.L. Occelli, S. Biz, A. Auroux, G.J. Ray, Micropor. Mesopor. Mater. 26 (1998) 193.
[31] Q. Zhang, Y. Wang, S. Itsuki, T. Shishido, K. Takehira, J. Mol. Catal. A: Chem. 188 (2002) 189.
[32] F.A. Cotton, G. Wilkinson, Advanced Inorganic Chemistry, Wiley Eastern Private Limited, New Delhi, 1966.
[33] S. Velu, N. Shah, T.M. Jyothi, S. Sivasankar, Micropor. Mesopor. Mater. 33 (1999) 61.
[34] F. Molella, J.M. Gallardo-Amores, M. Baldi, G. Busca, J. Mater. Chem. 8 (1998) 2525.
[35] J. Xu, A. Luan, T. Wasowiscz, L. Kevan, Micropor. Mesopor. Mater. 22 (1998) 179.
[36] Z. Levi, A.M. Raitsimring, D. Goldfrab, J. Phys. Chem. 95 (1991) 7830.
[37] Herman Pines, The Chemistry of Catalytic Hydrocarbon Conversions, Academic Press, London, 1981, p. 241.
[38] S. Vetrivel, A. Pandurangan, Catal. Lett. 95 (2004) 167.
[39] E. Baciocchi, F. d' Acunzo, C. Galli, M. Loele, J. Chem. Soc., Chem. Commun. (1995) 429.
[40] G. De, B. Karmakar, D. Ganfuli, J. Mater. Chem. 10 (2000) 2289.